PHYSICAL REVIEW B, VOLUME 65, 140503(R)

Vortex states and magnetization curve of square mesoscopic superconductors

A. S. Mel'nikov,[1,2] I. M. Nefedov,[1] D. A. Ryzhov,[1,*] I. A. Shereshevskii,[1] V. M. Vinokur,[2] and P. P. Vysheslavtsev[1]
[1] *Institute for Physics of Microstructures, Russian Academy of Sciences, 603950, Nizhny Novgorod, GSP-105, Russia*
[2] *Argonne National Laboratory, Argonne, Illinois 60439*
(Received 13 December 2001; published 22 March 2002)

The structure of the vortex states in a square mesoscopic superconductor is analyzed in detail using the numerical simulation within the time-dependent Ginzburg-Landau (TDGL) theory. Various vortex states (vortices, vortex molecules, multiquanta vortices) are observed and the magnetization curve is obtained. Different changes in vortex structures are identified with the peculiarities on the magnetization curve. Stability of a state consisting of vortices and antivortices is discussed.

DOI: 10.1103/PhysRevB.65.140503 PACS number(s): 74.25.Ha, 74.60.Ec

There has been an exciting development[1] in the study of magnetic properties of mesoscopic superconductors initiated in pioneering works.[2–5] Small few fluxoid superconductors (FFS) reveal the exotic vortex formations–multiquanta vortices and vortex molecules–that can transform one into another via first or second order phase transitions. These exotic states appearing in small coherence length-size samples[2–5] are due to screening currents pushing vortices to the center of the sample. Thus one should expect the resulting vortex configurations to be very sensitive to the geometry of the sample. Indeed, Chibotaru *et al.*[1] showed that the conflict between, for example, the fourfold symmetry of the square sample and the three-quanta vortex configuration may result in the appearance of complex vortex-antivortex configurations (four vortices + one centered antivortex) in the vicinity of upper critical magnetic field.

While numerical studies of the vortex states in mesoscopic superconductors explained fairly well many of the observed features of FFS of different geometries, several fundamental questions, in particular, the mechanism of multiquanta vortex dissociation and the role of symmetry effects in formation of particular vortex configurations remain open. In our work we develop a regular numerical description of the vortex state of FFS, based on the time-dependent Ginzburg-Landau (TDGL) theory and outline the symmetry approach to analytical studies of vortex molecules and complexes. Our simulations provide a possibility for detailed investigation of the nonlinear regime at low fields (far below the upper critical field). A large number of possible metastable states in the system is known to result in a strong dependence of vortex configurations on the initial conditions. In this case the evolution of the system with a change in magnetic field can be extremely sensitive to the details of the dynamic model. The use of the gauge-invariant time-dependent approach allows us to control the dynamics of phase transitions between the vortex states, which is important for the analysis of the magnetization curve in realistic experimental conditions. In particular, our TDGL simulations allowed us to visualize the changes in the vortex arrangement and obtain different stationary vortex states in a square superconductor, and enables us to identify modifications in vortex arrangement with the peculiarities on the magnetization curve and its derivatives. Finally, we discuss a possibility of coexistence of vortices and antivortices in mesoscopic superconductors.

The model. We investigate the structure of the vortex states (such as separated vortices, vortex molecules and multiquanta vortices) in a mesoscopic square superconductor, using the free energy functional for the order parameter (OP):

$$F=\int_S\left[a(T)|\Psi|^2+\frac{b}{2}|\Psi|^4+\frac{\hbar^2}{4m^*}\left|\left(\nabla-\frac{2\pi i}{\Phi_0}\mathbf{A}\right)\Psi\right|^2\right]dx\,dy, \tag{1}$$

where $a(T)=\alpha(T-T_c)$, T_c is the critical temperature, m^* is the effective mass of electron, $\Phi_0=\pi\hbar c/e$ is the flux quantum. Hereafter we use the following dimensionless units: $|\Psi_0|=\sqrt{|a|/b}$ for the order parameter (i.e., $|\Psi|=1$ in a bulk superconductor with $H=0$), $\xi=\sqrt{\hbar^2/(4m^*|a|)}$ for the length, $4ea^2\xi/(\hbar b)$ for the current density [i.e., the dimensionless depairing current density $j_c=2/(3\sqrt{3})$], $\Phi_0/(2\pi\xi)$ for the **A** field [i.e., the unit of magnetic field and local magnetization is $H_{c2}=\Phi_0/(2\pi\xi^2)$]. The dimensionless form for the superconducting current density is

$$\mathbf{j}=Im[\Psi^*(\nabla-i\mathbf{A})\Psi].$$

The magnetic field is perpendicular to the sample. We consider the sample of the size $L\ll\lambda_{eff}$ (λ_{eff} is the effective penetration depth of magnetic field). This allows to neglect the contributions to the magnetic field from supercurrents and thus to exclude Maxwell equations.

Calculations. We calculate the OP distribution from the TDGL equations sequentially for different values of the magnetic field starting with $H=0$ with a step $\Delta H=0.01$.

The dimensionless TDGL equations read

$$u\left(\frac{\partial}{\partial t}+i\Phi\right)\Psi=\Psi-|\Psi|^2\Psi+(\nabla-i\mathbf{A})^2\Psi,$$

$$\nabla^2\Phi=-\frac{i}{2}u\left[\Psi^*\left(\frac{\partial}{\partial t}+i\Phi\right)\Psi-\text{c.c.}\right]. \tag{2}$$

Hereafter we use the units $\hbar^2\sigma_n b/(8e^2a^2\xi^2)$ for time and $4ea^2\xi^2/(\hbar\sigma_n b)$ for electric potential. Here σ_n is the normal conductivity, u is the dimensionless characteristic time scale of the TDGL theory. The Laplace equation for electric po-

tential Φ results from the continuity equation that has the following dimensionless form: $div(\mathbf{j_s}-\nabla\Phi)=0$.

We approximated Eq. (2) on a rectangular grid on the (x,y) plane. The axes are chosen to be parallel to the sample edges. In order to save the gauge invariance of the difference equations the space differential operator $(\nabla-i\mathbf{A})$ was approximated in the same way as in Ref. 6. The evolution equations (2) are solved by the explicit Euler method using Fourier approach[7] allowing for a fast solution of the Neumann problem. Note that the difference equations yield a zero electrical potential in a stationary state. This allows us to determine the precise moment when the stationary state is reached.

To detect the vortex on the grid cell corresponding to the certain grid node (x_i,y_j), we use the following criterion:

$$\arg(\Psi^*_{i,j}\Psi_{i,j+1})+\arg(\Psi^*_{i,j+1}\Psi_{i+1,j+1}) + \arg(\Psi^*_{i+1,j+1}\Psi_{i+1,j})+\arg(\Psi^*_{i+1,j}\Psi_{i,j})=2\pi N. \tag{3}$$

Here $\Psi_{i,j}=\Psi(x_i,y_j)$ is the complex grid function, $\arg(\Psi)$ is the argument of the complex number $\Psi_{i,j}$, belonging to the interval $(-\pi,\pi]$. If integer $N=\pm1$, there is a vortex with the winding number N. If integer $N=0$, there are no vortices in the cell. It should be noted that there are no multiquanta vortices for the rectangular *grid* approximation of Eq. (2), i.e., $\max|N|=1$ for each grid cell. Nevertheless, the multiquantum vortex appears in the grid model as an ensemble of singly-quantized vortices in the neighboring cells.

Most calculations were performed on the grid with $\Delta x=\Delta y=\xi/16$ for $L=8\xi$ and with $\Delta x=\Delta y=\xi/64$ for $L=4\xi$. The numerical factor u is determined by the pair-breaking mechanism. If the lack of the energy gap is connected with strong electron-phonon relaxation, then $u=5.79$ (Ref. 8). For superconductors with a high concentration of magnetic impurities $u=12$ (Ref. 9). The time step was in the range 0.005–0.01 of dimensionless units.

For all values of magnetic field the average magnetization was calculated as

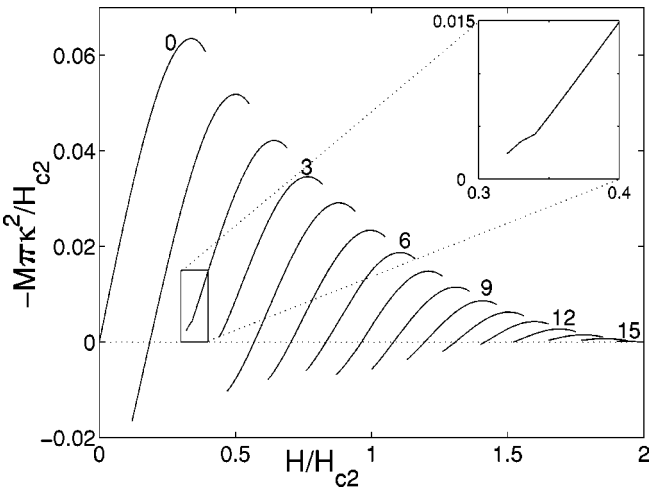

FIG. 1. The magnetization curve $M(H)$ for $L=8\xi$. The numbers near the branches are guides for the eye and denote the total vorticity $\mathcal{N}$ in the sample.

$$\mathbf{M}=\frac{1}{S}\int_S\frac{[\mathbf{r}\times\mathbf{j}]}{8\pi\kappa^2}dx\,dy,$$

where $\kappa=\lambda/\xi$ is the Ginzburg-Landau parameter, and S is the sample area.

The total vorticity is defined as

$$\mathcal{N}=\oint_\Gamma\nabla(\arg\Psi)d\Gamma/(2\pi),$$

where Γ is the perimeter of sample, $\arg(\Psi)$ is the argument of the complex function Ψ (i.e., the order parameter phase). In the absence of either multiquanta vortices or antivortices, the $\mathcal{N}$ simply represents the number of vortices (singularities of Ψ) in a superconductor. The change in the total vorticity upon varying the magnetic field describes the entrance (or exit) of vortices.

The introduction of a small, $0.01\xi\times0.01\xi$, defect (a piece of a normal metal) leaves the OP and the current distributions almost undisturbed. Yet such a defect slightly disturbs

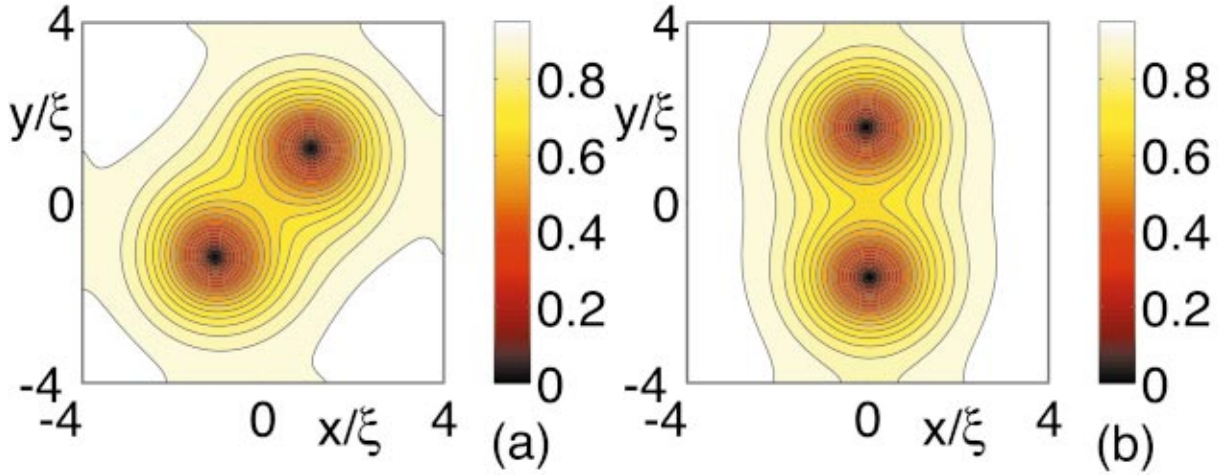

FIG. 2. (Color) Vortex rearrangement scenario for $\mathcal{N}=2$. Contour plots of the $|\Psi|$ for $H=0.34$ (a) and $H=0.33$ (b).

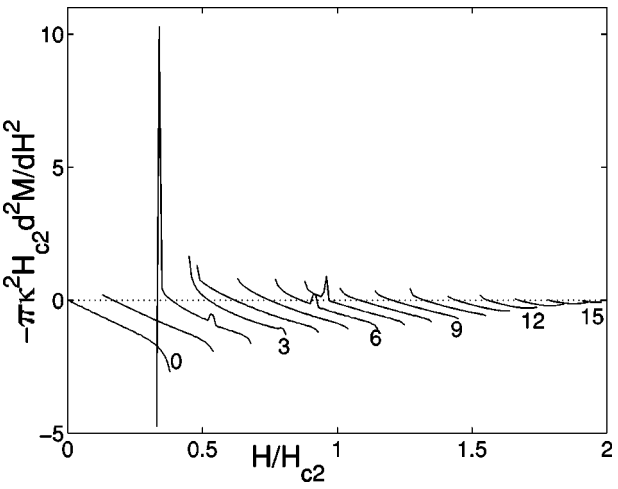

FIG. 3. Dependence d^2M/dH^2 on H for $L=8\xi$. The numbers near the branches are guides for the eye and denote the total vorticity $\mathcal{N}$ in the sample.

the fourfold symmetry of the *scheme of numerical simulation*, which allows us to obtain the branches on the magnetization curve with an odd total vorticity, whereas a perfect fourfold symmetric sample provides only even-$\mathcal{N}$ branches (vortices entered into the sample simultaneously from the two opposite edges).

We observe the Meissner state when the total vorticity $\mathcal{N}=0$, and sequential entries of vortices, which produces different branches with different total vorticities on the magnetization curve (Fig. 1). We have obtained different vortex states and studied their behavior under a changing magnetic field. One interesting result was observed for $\mathcal{N}=2$. We have observed that the cusp on the 2-vortex branch is caused by rearrangement of two vortices. At a higher magnetic field vortices are arranged along the sample diagonal [Fig. 2(a)], at lower field the vortices get rearranged along the sample edge [Fig. 2(b)].

Also we have observed peaks on some branches on the dependence d^2M/dH^2 (see Fig. 3). Such peaks are caused by

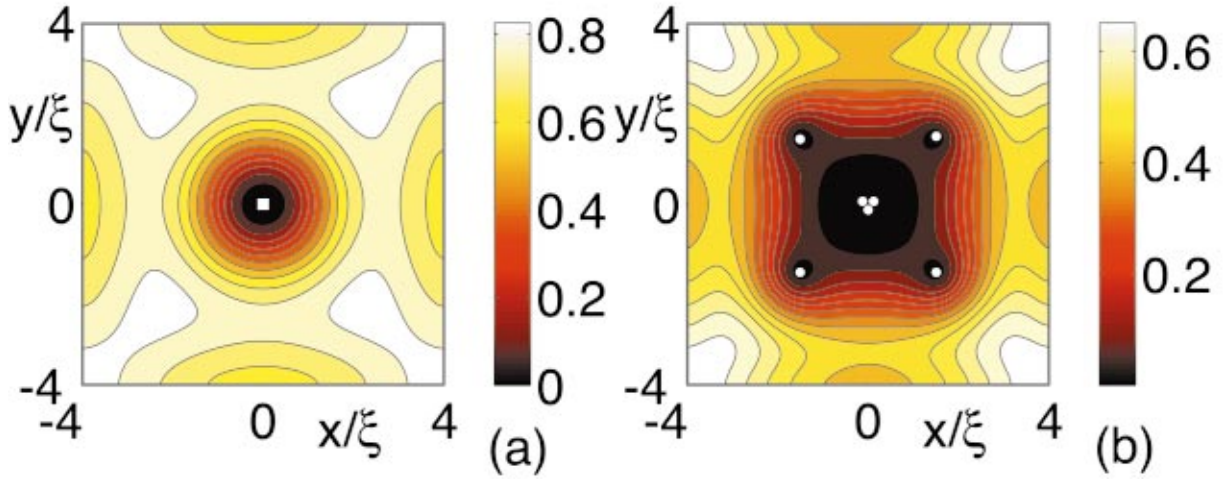

FIG. 4. (Color) Contour plots of the $|\Psi|$ for (a) double-quantized vortex ($H=0.65$) and (b) $3\Phi_0$-molecule situated in the center ($H=1.26$, $\mathcal{N}=7$). The white circles denote singly-quantized vortices, the white square denotes the double-quantized vortex.

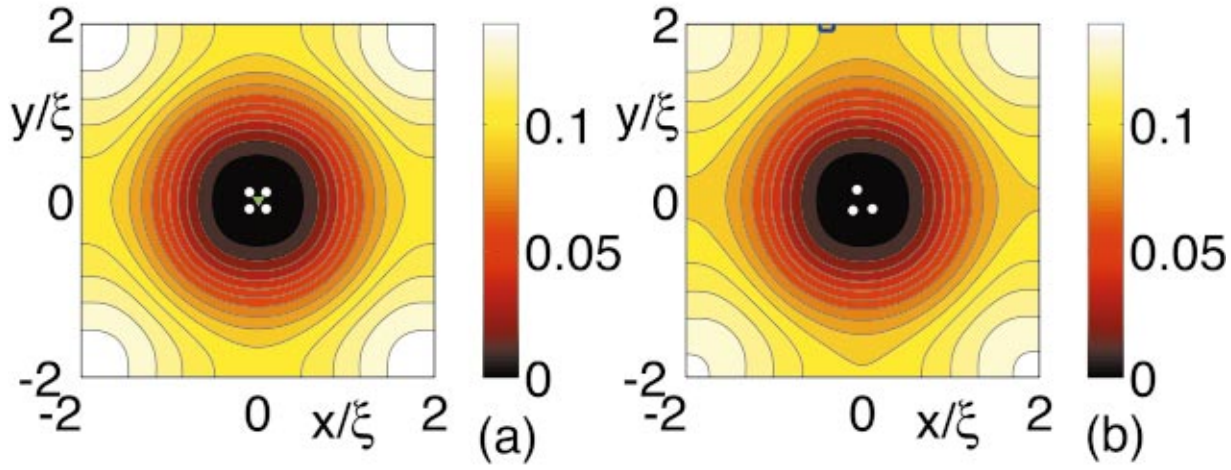

FIG. 5. (Color) The contour plot of the $|\Psi|$ for $H=2.15H_{c2}$, $L=4\xi$ in an ideal square (a) and in a square with a small defect (b) of the size $0.16\xi\times0.08\xi$ shown by the blue rectangle on the upper edge. The white circles denote the vortices, the green triangle denotes the antivortex.

dissociation of three-vortex molecule (for $\mathcal{N}=7$), and by decay of the double-quantized vortices (for $\mathcal{N}=2$ and $\mathcal{N}=6$) which are situated in the center of specimen (see Fig. 4).

In a recent work[1] Chibotaru *et al.* report obtaining a vortex arrangement with an antivortex for $\mathcal{N}=3$ at the upper critical field H_{c3} in a square mesoscopic superconductor. At the certain values of the sample size ($3.8<L/\xi<4.5$) they have found a vortex state with four vortices on the diagonals and one antivortex in the center of the square. We obtained such a vortex state [Fig. 5 (a)] for the sample with $L=4\xi$ near the upper critical field ($H=2.15H_{c2}$, $H_{c3}\simeq 2.18H_{c2}$). Here H_{c2} is the upper critical field in a bulk superconductor.

We conjecture that this vortex configuration of a small size $0.19\xi\times 0.19\xi$ is realization of a triple-quantized vortex in a square superconductor. Let us consider a triple-quantized vortex within the expansion in series of harmonics $\Psi=\Sigma R_n(r)e^{in\theta}$. As emphasized in Ref. 1, the fourfold symmetry of a sample strongly influence the vortex arrangement, therefore, the dominant term for the triple-quantized vortex $R_3(r)e^{3i\theta}$ generates additional terms $R_{3+4m}(r)e^{(3+4m)i\theta}$ ($m=0,\pm 1,\pm 2,\ldots$). Since at small distances $R_n\propto r^{|n|}$, the OP $\Psi\simeq\alpha(r/L_H)e^{-i\theta}+(r/L_H)^3e^{3i\theta}$ (where $L_H=\sqrt{\hbar c/(eH)}\lesssim\xi$ is the magnetic length in the vicinity of the upper critical field), which yields one antivortex in the center and four vortices around the antivortex in the vertices of a square. The generation of the R_{-1} harmonic is necessary to satisfy the boundary condition at the sample edge and can be considered as a superposition of four Gaussian-like nuclei with centers near the square boundary and characterized by four different phases $\varphi_n=-3\pi n/2$ ($n=0,1,2,3$). Close to the square center such a superposition gives us the R_{-1} harmonic with $\alpha\sim L/L_H\exp(-(L/L_H)^2/4)$. So we can conclude that the size r_0 of such vortex-antivortex configuration is naturally determined by the factor ξ/L and appears to be much smaller than the coherence length even for $L=4\xi$: $r_0/L_H\sim\sqrt{L/L_H}\times\exp(-(L/L_H)^2/8)$.

In order to examine a stability of such a vortex state to fourfold symmetry distortions we set a small rectangular defect of a normal metal asymmetrically on one edge of a sample. Starting with the size $0.01\xi\times 0.02\xi$ we have increased the square of defect and observed distortion of the vortex state mentioned above: the antivortex came close to one of the vortices and when the size of defect became $0.16\xi\times 0.08\xi$ this vortex-antivortex pair annihilated [Fig. 5(b)]. Note that all through the above calculations the space resolution was quite high: $\Delta x=\Delta y=\xi/64$. Thus we come to a conclusion that this vortex configuration with one antivortex and four vortices is very sensitive to distortions of the symmetry, which may be caused by defects or fluctuations.

We would like to point out that similarly to the nontrivial structure of a triple-quantized vortex in a square, a double-quantized vortex in a triangle also consists of an antivortex and three vortices.[10] This vortex arrangement can be described in the vicinity of the core as follows: $\Psi\simeq\alpha_2 r^2e^{2i\theta}+\alpha_{-1}re^{-i\theta}$ since according to the boundary conditions the dominant term $R_2(r)e^{2i\theta}$ generates additional terms $R_{2+3m}(r)e^{(2+3m)i\theta}$ ($m=0,\pm 1,\pm 2,\ldots$).

In conclusion, we have derived different vortex states in a square mesoscopic superconductor using numerical simulations of the time-dependent Ginzburg-Landau (TDGL) equations and calculated the corresponding magnetization curves. We have identified different modifications of the vortex arrangement with peculiarities in the magnetization curves and their derivatives. In particular, we identified the cusps on the second derivative of the magnetization curve with the vortex molecule dissociation and the decay of a double-quantized vortex. We have found that a rearrangement of two vortices leads to a kink on the 2-vortex branch of the magnetization curve.

We have also found that a triple-quantized vortex can be realized in a square mesoscopic superconductor near the upper critical field H_{c3} as a vortex state with one antivortex and four vortices just as a double-quantized vortex in a triangle superconductor is realized as one antivortex and three vortices. Such vortex states are very sensitive to any distortion of the symmetry, like defects or fluctuations. We have presented a symmetry approach that enabled us to evaluate analytically the conditions for the existence of the complex vortex-antivortex configurations.

We thank V. Moshchalkov for useful discussions. This work was supported by the U.S. DOE, Office of Science under Contract No. W-31-109-ENG-38, NATO Collaborative Linkage Grant No. PST.CLG.978122, Russian Foundation for Fundamental Research, Grant Nos. 99-02-16188, 00-02-16158, 01-02-06494, and by Russian Academy of Sciences under the Program ''Quantum Macrophysics.''

*Email address: ryzhov@ipm.sci-nnov.ru

[1] L.F. Chibotaru, A. Ceulemans, V. Bruyndoncx, and V.V. Moshchalkov, Nature (London) **408**, 833 (2000).

[2] G. Boato, G. Gallinaro, and C. Rizzuto, Solid State Commun. **3**, 173 (1965); D.S. McLachlan, *ibid.* **8**, 1589 (1970); **8**, 1595 (1970); Phys. Rev. Lett. **23**, 1434 (1969).

[3] A.K. Geim, S.V. Dubonos, I.V. Grigorieva, K.S. Novoselov, F.M. Peeters, and V.A. Schweigert, Nature (London) **390**, 259 (1997); **396**, 144 (1998); **407**, 55 (2000).

[4] S.V. Yampolskii and F.M. Peeters, Phys. Rev. B **62**, 9663 (2000).

[5] A.K. Geim, S.V. Dubonos, J.J. Palacios, I.V. Grigorieva, M. Henini, and J.J. Schermer, Phys. Rev. Lett. **85**, 1528 (2000).

[6] K.H. Lee and D. Stroud, Phys. Rev. B **43**, 5280 (1991).

[7] I.A. Shereshevskii, J. Nonlinear Math. Phys. **8**, 446 (2001).

[8] R.J. Watts-Tobin, Y. Krahenbuhl, and L. Kramer, J. Low Temp. Phys. **42**, 459 (1981).

[9] L.P. Gor'kov and G.M. Eliasberg, Zh. Éksp. Teor. Fiz. **54**, 612 (1968) [Sov. Phys. JETP **27**, 328 (1968)].

[10] L.F. Chibotaru, A. Ceulemans, V. Bruyndoncx, and V.V. Moshchalkov, Phys. Rev. Lett. **86**, 1323 (2001).